



HAL
open science

Involvement of Type I Interferon Signaling in Muscle Stem Cell Proliferation During Dermatomyositis

Laure Gallay, Cécile Fermon, Lola Lessard, Michèle Weiss-Gayet, Sébastien Viel, Nathalie Streichenberger, Armelle Corpet, Rémi Mounier, Cyril Gitiaux, Guy Mouchiroud, et al.

► **To cite this version:**

Laure Gallay, Cécile Fermon, Lola Lessard, Michèle Weiss-Gayet, Sébastien Viel, et al.. Involvement of Type I Interferon Signaling in Muscle Stem Cell Proliferation During Dermatomyositis. *Neurology*, 2022, 98 (21), pp.e2108-e2119. 10.1212/WNL.0000000000200271 . hal-04830900

HAL Id: hal-04830900

<https://hal.science/hal-04830900v1>

Submitted on 11 Dec 2024

HAL is a multi-disciplinary open access archive for the deposit and dissemination of scientific research documents, whether they are published or not. The documents may come from teaching and research institutions in France or abroad, or from public or private research centers.

L'archive ouverte pluridisciplinaire **HAL**, est destinée au dépôt et à la diffusion de documents scientifiques de niveau recherche, publiés ou non, émanant des établissements d'enseignement et de recherche français ou étrangers, des laboratoires publics ou privés.



Distributed under a Creative Commons Attribution - NonCommercial - NoDerivatives 4.0 International License

Involvement of Type-I Interferon signaling in muscle stem cell proliferation during dermatomyositis

Author(s):

Laure Gallay, PhD, MD^{1,2}; Cécile Fermon, MD^{1,2}; Lola Lessard, MD^{1,3}; Michèle Weiss-Gayet, PhD¹; Sébastien Viel, PhD, MD^{4,5}; Nathalie Streichenberger, PhD, MD^{1,6}; Armelle Corpet, PhD¹; Rémi Mounier, PhD¹; Cyril Gitiaux, PhD, MD^{7,8}; Guy Mouchiroud, PhD¹; Bénédicte Chazaud, PhD¹

Equal Author Contributions:

co-senior authors Guy Mouchiroud Bénédicte Chazaud

Corresponding Author:

Bénédicte Chazaud

benedicte.chazaud@inserm.fr

Affiliation Information for All Authors: 1 Institut NeuroMyoGène, Université Claude Bernard Lyon 1, Univ Lyon, CNRS UMR 5310, Inserm U1217, Lyon, France. 2 Service de Médecine Interne, Hospices Civils de Lyon, Lyon, France 3 Service d'Electroneuromyographie et pathologies neuromusculaires, Hospices Civils de Lyon, Lyon, France. 4 Service d'Immunologie biologique, Hospices Civils de Lyon, Lyon, France 5 Centre International de Recherche en Infectiologie, Université Claude Bernard Lyon 1, Univ Lyon, CNRS UMR 5308, Inserm U1111, Lyon, France. 6 Service d'Anatomopathologie, Hospices Civils de Lyon, Lyon, France. 7 Centre de référence pour les maladies neuromusculaires, Département de Neurophysiologie Pédiatrique, Hôpital Necker-Enfants Malades, APHP, Paris, France 8 Institut Mondor de Recherches Biomédicales, Université Paris-Est, Inserm U955, Créteil, France.

Contributions:

Laure Gallay: Drafting/revision of the manuscript for content, including medical writing for content; Major role in the acquisition of data; Study concept or design; Analysis or interpretation of data

Cécile Fermon: Major role in the acquisition of data; Analysis or interpretation of data

Lola Lessard: Major role in the acquisition of data; Analysis or interpretation of data

Michèle Weiss-Gayet: Major role in the acquisition of data; Analysis or interpretation of data

Sébastien Viel: Major role in the acquisition of data; Analysis or interpretation of data

Nathalie Streichenberger: Major role in the acquisition of data

Armelle Corpet: Analysis or interpretation of data

Rémi Mounier: Drafting/revision of the manuscript for content, including medical writing for content; Analysis or interpretation of data

Cyril Gitiaux: Drafting/revision of the manuscript for content, including medical writing for content; Major role in

the acquisition of data; Analysis or interpretation of data

Guy Mouchiroud: Drafting/revision of the manuscript for content, including medical writing for content; Major role in the acquisition of data; Study concept or design; Analysis or interpretation of data

Bénédicte Chazaud: Drafting/revision of the manuscript for content, including medical writing for content; Major role in the acquisition of data; Study concept or design; Analysis or interpretation of data

Number of characters in title: 88

Abstract Word count: 329

Word count of main text: 4076

References: 50

Figures: 5

Tables: 1

Supplemental: - Response to reviewer's comments - Supplemental figures and table - Strobe checklist - manuscript with track changes - coauthor's agreement for an additional co-author

Statistical Analysis performed by: t-test ANOVA

Search Terms: [132] Autoimmune diseases, [185] Muscle disease

Acknowledgements: We thank the Laboratoire de Culture cellulaire du Service de Génétique et Biologie Moléculaire de l'Hôpital Cochin, Paris.

Study Funding: Association Française contre les Myopathies-Telethon (Alliance MyoNeurALP) Société Française de Médecine Interne (support for LG) Inserm (poste d'accueil for LG) Fondation pour la Recherche Médicale (fellowship for LL)

Disclosures: All authors report no disclosures relevant to the manuscript

Abstract

Background and objective: The idiopathic inflammatory myopathy Dermatomyositis (DM) is an acquired disease that combines muscle, lung and skin impairments. DM patients show a wide range of severity of proximal skeletal muscle weakness, associated with inflammatory infiltrates, vasculitis and capillary dropout, perifascicular myofiber atrophy. Moreover, DM muscles show signs of muscle regeneration. Since muscle stem cells (MuSCs) are responsible for myofiber repair, we asked whether the proliferative properties of muscle stem cells (MuSCs) are altered in DM muscle. We investigated the role of type-I interferon (IFN-I) in this process since DM is associated with sustained inflammation with high IFN-I levels.

Methods: MuSCs isolated from normal, adult and juvenile DM muscles were grown in culture and were analyzed *in vitro* for their proliferating properties, their myogenic capacities and their senescence. Gain and loss of function experiments were performed to assess the role of IFN-I signaling in the proliferative capacities of MuSCs.

Results: MuSCs derived from 8 DM adult patients (DM-MuSCs) (5 severe form and 3 mild form, established from histological evaluation), from 3 juvenile DM patients and from normal muscle were used to analyze their myogenesis *in vitro*. DM-MuSCs exhibited strongly reduced proliferating capacities as compared with healthy MuSCs (-31 to -43% for severe and mild DM, respectively), leading to poor myotube formation (-36 to -71%). DM-MuSCs were enriched in senescent, beta-galactosidase positive cells, explaining partly the proliferation defect. Gain and loss of function experiments were performed to assess the role of IFN-I on the proliferative capacity of MuSCs. High concentrations of IFN-I decreased the proliferation of healthy MuSCs. Similarly, conditioned-medium from DM-MuSCs decreased the proliferation of healthy MuSC (-15 to -22%), suggesting the delivery of an autocrine effector. Then, pharmacological blockade of the IFN signaling (using ruxolitinib or anti-IFN-receptor antibodies) in DM-MuSCs rescued their proliferation up to the control values.

Discussion: These results show that autocrine IFN-I signaling prevents MuSC expansion, leading to muscle repair deficit. This process may explain the persistent muscle weakness observed in severe DM patients.

Introduction

Dermatomyositis (DM), the most frequent subgroup of idiopathic inflammatory myopathies, is an acquired disease that combines clinicopathological muscle, lung and skin impairments of various severity. DM patients show a wide range of severity of proximal skeletal muscle weakness, associated with inflammatory infiltrates, vasculitis and capillary dropout, and a myofiber atrophy that is preferentially localized in perifascicular areas^{1,2}. DM occurs in adults and children and is designated juvenile DM (jDM) in the latter case. Identification of myositis specific auto-antibodies promoted investigations towards humoral immunopathogenesis. However, DM pathogenesis remains partially understood, and seems to combine many factors, including genetic background, environmental factors, metabolism dysfunction, as well as dysregulation of adaptive and innate immunity³. Through histologic and transcriptomic analyses of DM muscle samples, type 1 interferon (IFN-I, including IFN α and IFN- β) was identified as a key element in DM^{1, 4, 5} and its expression levels were reported to correlate with the disease activity and severity^{6, 7}. Notwithstanding the use of various immunosuppressive drugs to extinguish the autoimmune reaction, the disease follows in most cases a chronic course with rare outcomes of recovery of the initial strength, and some DM patients sustain muscle atrophy and fat replacement of muscle tissue, leading to loss of muscle strength and handicap⁸⁻¹⁰.

Histological observation of skeletal muscle biopsies shows patterns of both muscle damage and muscle regeneration of various extent in all DM patients, indicating that muscle regeneration is an active process during DM¹¹. Post-injury skeletal muscle regeneration is a well-understood process leading to the *ad integrum* restoration of damaged myofibers, thanks to the properties of satellite cells, or Muscle Stem Cells (MuSCs). Laying along the myofiber as quiescent cells in resting muscle, MuSCs activate upon injury, and undergo adult myogenesis that encompasses expansion/proliferation, myogenic differentiation and eventually fusion to form new myofibers¹². This process is tightly controlled by the sequential expression of myogenic transcription factors in MuSCs and is also regulated by extracellular cues provided by the MuSC environment¹².

The involvement of IFN-I has been largely described in DM. We propose here a new focus on the process of muscle regeneration itself in DM pathogenesis, through the analysis of the intrinsic properties of MuSCs derived from patient's skeletal muscle. Given that DM patients exhibit features of chronic muscle damage and regeneration, we hypothesized that the intrinsic myogenic properties of MuSCs may be altered in DM. For the first time, MuSCs purified from DM patient's skeletal muscle were analyzed for their intrinsic myogenic capacities *in vitro*, with a focus on the first step of myogenesis that is proliferation. We showed that DM-MuSCs exhibited a deficit in proliferation. We also investigated the role of IFN-I in this process, and sought for a potential autocrine mechanism sustaining the proliferation deficit, through IFN-I, and explaining the failure in muscle regeneration observed in DM patients.

Methods

Case selection. Eight DM patients were identified through screening of the MYOLYON database (Hospices Civils de Lyon, France) that identifies Idiopathic Inflammatory Myopathies in accordance with the EULAR/ACR 2017 or 239th ENMC criteria 2018¹³. DM patients with available clinical data, histological samples, frozen muscle samples and MuSCs were selected. Exclusion criterion was immunosuppressive drug administration to the patient before muscle biopsy. Healthy controls (HC) MuSCs paired on sex and age were obtained from surgical waste of patients undergoing programmed knee or hip surgery (n = 5). None of the DM patients were on cytotoxic medication (in particular, statin) at the time of biopsy. Biopsies, made at the time of diagnosis, were obtained after institutionally approved protocol. Healthy controls (HC) MuSCs paired on sex and age were obtained from surgical waste of patients undergoing programmed knee or hip surgery. MuSCs were obtained from the Hospices Civils de Lyon cell bank (Cardiobiotec CRB-HCL AC2013-1867). Juvenile DM (jDM) patients (n=3) and aged-matched HC controls (n=3) were selected as previously described¹⁴.

Standard Protocol Approvals, Registrations, and Patient Consents. Written informed consent was obtained from all patients (or legal representative) for the use of their biopsy for research purposes. The whole procedure was handled by the Hospices Civils de Lyon cell bank and the Cochin Hospital Cell Bank, Paris.

Histology and immunohistology. Histological staining and immunohistochemistry of muscle sections (7 µm) included hematoxylin and eosin staining (HE), immunohistochemistry for endothelial cells (anti-CD31 antibody, M0823 Dako), MuSCs and regenerating myofibers (anti-CD56 antibody, NCL-CD56-1B6 Novocastra). All biopsy samples were blindly reviewed for clinical data, using the validated scoring tool for muscle biopsy evaluation in DM Patients (eTable 1). Visualization and quantification of MuSCs was performed after incubation with anti-Pax7 antibody (DSHB) revealed by a FITC-conjugated secondary antibody (Jackson

Immunoresearch). Slides were scanned using a Zeiss Axio Observer Z1 microscope. Image analyses were performed using ImageJ software. Quantification of Pax7^{pos} cells distinguished the perifascicular area (2 first rows of myofibers from the perimysium) and the rest of the fascicle.

MuSC culture. MuSCs were directly extracted by mechanic and enzymatic digestion from fresh muscle biopsies made at the time of diagnosis. After an expansion period, they were frozen and stored in liquid nitrogen at the hospital cell bank. After thawing, MuSCs were purified at the first passage of primary culture using anti-CD56 coated magnetic beads to obtain pure myogenic cell cultures as described previously¹⁴. Cell purity was checked by flow cytometry (BD FACSCanto II) using anti-CD56 antibodies (APC-conjugated anti-CD56 antibodies (BD Pharmingen #555518) and isotypic control (#555751)). MuSCs were cultured for a maximum of 4 passages in complete medium (Skeletal Muscle Cell Growth Medium [#23060 Promocell] supplemented with Mix C-39365 [Promocell] and heat-inactivated Fetal Bovine Serum [FBS, Sigma-Aldrich] 10%). Conditioned-medium was prepared from MuSCs cultured during 48h in growing medium. Medium was collected, centrifuged at 2,000 rpm and stored at -80°C until use.

Myogenesis assay. Analysis of myogenesis capacities of jDM- and DM-derived MuSCs was performed as follows: cells were seeded in 2 well-chambers (Lab-Tek, Nunc) at 3,000 cells/cm² in complete medium for 3 days, then they were switched to differentiation medium (Skeletal Muscle Cell Growth Medium [#23060 Promocell] supplemented with 10 µg/ml Insulin [Sigma-Aldrich] and FBS 0.5%) and cultured for 3 additional days. Proliferation was evaluated at day 3 at the end of the expansion phase using EdU incorporation for 6 h (kit EdU Click-it Alexa Fluor™ 488, Invitrogen). In some experiments, the proliferation assay was performed in conditioned medium (prepared as described above). Myogenic differentiation and fusion were evaluated at day 6. Terminal myogenic differentiation was assessed after immunolabeling for the transcription factor Myogenin (BD Pharmingen #556358 antibodies),

revealed using a biotinylated secondary antibody and DTAF-biotin (Jackson ImmunoResearch). Fusion was evaluated after desmin immunolabeling (Abcam ab32362), revealed by a Cy3-conjugated secondary antibody (Jackson ImmunoResearch). In all immunofluorescence experiments, cells were briefly incubated in Hoechst 33342 (Sigma-Aldrich) for nuclei visualization and slides were mounted using Fluoromount (Interchim). For each sample, 10-15 pictures were recorded at x20 magnification using an AxioImager Z1 Zeiss microscope. Proliferation index was defined as the number of EdU positive nuclei over the total number of nuclei, differentiation index was defined as the number of Myogenin positive nuclei over the total number of nuclei, and fusion index was calculated as the number of nuclei present in myotubes (>2 nuclei in the same desmin positive cell) over the total number of nuclei.

Modulation of the IFN-I pathway. HC-MuSCs were seeded in 2 well-chambers at 3,000 cells/cm² in complete medium for 6 h, time to adhere. In IFN-I activation experiments, medium was replaced by Advanced medium (Advanced RPMI 1640 medium [Gibco #12633] supplemented with Glutamax [Gibco #35050] and FBS 0.5%) containing or not increasing concentrations of human IFN- β -1a (10 to 1000 U/ml) (PBL assay #11415-1). In IFN-I inhibition experiments, DM-MuSCs were grown in complete medium in the presence of ruxolitinib (INCB018424, Invivogen #trl-rux at 2 μ M) or anti-Human Interferon Alpha/Beta Receptor Chain 2 (PBL assay science, #21385-1 at 5 μ l/ml). Concentrations were defined from ^{15, 16}. After 48 h of culture, proliferation assay was performed and analyzed as described above.

Cell cycle analysis. MuSCs were seeded in T75 flask at 3,000 cells/cm² in complete medium. After 4 days of culture, cells were harvested, washed and incubated with Hoechst 33342 at a final concentration of 10 μ g/ml then Pyronin Y was added at a final concentration of 2.5 μ g/ml, as previously described ¹⁷. Control included treatment with RNase (2 mg/ml,

Sigma-Aldrich). Cells were analyzed by flow cytometry (BD FACSCanto II) to determine G0, G1/S and G2/M phases.

Senescence analysis. Senescence was measured by flow cytometry using a protocol adapted from ¹⁸, evaluating the SA- β gal activity. MuSCs were seeded in T75 flask at 3,000 cells/cm² in complete medium. After 4 days of culture, cells were pretreated with bafilomycin A1 (Sigma-Aldrich, 100 nM) for 1 h to induce lysosomal alkalization, followed by 1 h incubation with 5-dodecanoylaminofluorescein di- β -D-galactopyranoside (C12FDG) (33 μ M, Sigma-Aldrich), a fluorogenic substrate for β -galactosidase. Cells were washed, harvested, resuspended in ice-cold PBS and immediately analyzed by flow cytometry (BD FACSCanto II).

MuSC IFN signature. The expression of 6 Interferon Sensitive Genes (ISGs) was evaluated according to the Nanostring method described in ¹⁹: SIGLEC1 (sialic acid binding Ig like lectin 1), IFI27 (interferon alpha inducible protein 27), IFI44L (interferon induced protein 44 like), IFIT1 (interferon induced protein with tetratricopeptide repeats 1), ISG15 (interferon-stimulated gene 15) and RSAD2 (radical S-adenosyl methionine domain containing 2).

Statistics. Results were analyzed using t-test or ANOVA and a p-value below 0.05 was considered as statistically significant.

Data Availability. Anonymized data not published within this article will be made available by request from any qualified investigator.

Results and Discussion

Additional data are listed in eTable 1 and eFigures 1, 2, 3 in the Supplement.

Case selection

DM diagnosis was confirmed after histological analysis of the muscle biopsy if at least 2 of the 3 following criteria were present: inflammatory infiltrates, capillary dropout and overexpression of Major Histocompatibility Complex-1 (MHC-1) by myofibers (eTable 1). DM severity score was set up using a four-domain analysis, adapted from²⁰ (eTable 1). Severity score (Table 1) delineated 2 distinct histological subgroups: mild DM (mDM) and severe DM (sDM), with a severity score <7 for mDM and >13 for sDM, resulting in the selection of 8 patients for the present study (Table 1).

mDM muscle showed limited DM features such as few perivascular inflammatory infiltrates, moderate perifascicular atrophy, focal capillary dropout (visible after CD31 immunolabeling), and sparse myofibers undergoing regeneration (positive for CD56/NCAM) (Figure 1). In contrast, sDM muscle exhibited important myofiber damage featuring heterogeneity in myofiber size, severe perifascicular atrophy, necrosis and myophagocytosis, abundant inflammatory infiltrates, fibrosis, multiple areas of capillary dropout associated with atrophic areas and strong CD56 expression in perifascicular myofibers (Figure 1). Moreover, a simplified clinical correlation was made (Table 1). Globally, creatine kinase level and muscle weakness appeared consistent with the mild or severe status of DM patients. Persistence of muscle weakness over the years was observed only in sDM patients (Table 1).

Alteration of myogenic properties of MuSCs in DM

The expression of CD56 in myofibers indicates that DM patient's muscles undergo post-damage muscle regeneration. A previous *in vivo* analysis of DM muscle has shown that the number of cells expressing myogenic markers, including Pax7 (quiescent and activated MuSCs), MyoD (activated MuSCs) and Myogenin (differentiating MuSCs), is increased in myositis, including DM²¹. Accordingly, the number of newly formed myofibers (positive for

neonatal myosin and CD56/NCAM) is also increased as compared with normal muscle ²¹. Here, we investigated the number of MuSCs in Healthy Control (HC) and sDM muscle *via* Pax7 expression, which specifies both quiescent and expanding MuSCs. Because muscle damage and regeneration localize in perifascicular areas in DM ² (Figure 1), we analyzed perifascicular and intrafascicular areas separately (eFigure 1). The number of MuSCs (Pax7^{pos}) was increased by 206% in perifascicular areas in DM *versus* HC muscle, while it was similar to the control values inside fascicles (Figure 2). It was previously shown that together with the presence of CD56^{pos} myofibers, an increased number of Pax7^{pos} cells indicates MuSC activation in attempt to regenerate damaged myofibers in perifascicular areas, which is the place of active disease in DM ². Although not quantified, similar findings were observed in jDM with an increased number of Pax7^{pos} cells at the site of perifascicular atrophy ²².

Upon activation, adult MuSCs follow the myogenesis program to replace damaged myofibers, a process that is spontaneously recapitulated *in vitro*. *In vitro* myogenesis includes 3 major steps that are proliferation, commitment into terminal myogenic differentiation and fusion to form multinucleated myotubes that prefigure myofibers (Figure 3A). Proliferation assay (EdU incorporation in growing cells) showed that sDM-MuSCs and mDM-MuSCs exhibited a strong deficit in their proliferative capacities as compared with HC-MuSCs (-43 and -31%, respectively) (Figure 3B, eFigure 2A). In accordance with our results, it was previously shown that MuSCs isolated from DM and polymyositis muscles exhibit a slower growth as compared with normal MuSCs ²³.

After their expansion phase, MuSCs were transferred in differentiation medium and were analyzed for their differentiation and fusion capacities (Figure 3A). Figure 3C (and eFigure 2A) shows that terminal differentiation, assessed by the expression of the myogenic regulatory factor Myogenin, was strongly decreased in sDM-MuSCs as compared with HC-MuSCs (-68%), while mDM-MuSCs did not present a defect in their commitment into myocytes. In addition, the fusion capacities of both sDM and mDM were strongly altered as compared with those of HC-MuSCs, with a decrease of 71 and 36 % of their fusion index,

respectively (Figure 2D, eFigure 2A), leading to a decrease of the number of myotubes that were formed (eFigure 2B) and of the formation of large myotubes (eFigure 2C). Because MuSCs were purified using CD56 magnetic beads, leading to a range of 83 to 98% of CD56^{pos} cells in the resulting population, we checked whether impaired proliferation and myogenesis were due to the presence of the 2 to 17% of non-myogenic cells in the cultures. Correlation analyses showed that culture purity had no impact on the capacity of MuSCs to proliferate (eFigure 2D) and to differentiate (eFigure 2E). In the protocol used, MuSCs were expanded before stimulation for myogenic differentiation. Therefore, the defect in proliferation may impact on the next steps that are differentiation and fusion. Indeed, correlation analyses showed that the low proliferation capacities of the cells did correlate with a low differentiation (eFigure 2F), and even further low fusion capacities (eFigure 2G). While these results cannot rule out an autonomous defect in differentiation and fusion *per se* in DM-MuSCs, they show that the low proliferation rate observed in DM-MuSCs impacted on their whole myogenesis properties. Finally, we showed that in the context of juvenile DM (jDM), jDM-MuSCs also exhibited a decrease in their proliferative capacities (-54% as compared with age-matched HC-MuSCs) (**Figure 3E**).

Altogether, these results support the presence of activated MuSCs in diseased areas of skeletal muscle of DM patients, associated with altered intrinsic myogenic properties of MuSCs that may account for the sustained patient muscle weakness.

Increased senescence of MuSCs in DM

The proliferation defect observed in DM-MuSCs may reflect alterations of cell cycle and/or senescence. Cell cycle status of MuSCs was investigated using Pyronin Y/Hoechst staining after synchronization of the cells as described in ¹⁷. No significant changes in the distribution of MuSCs in the various phases of the cell cycle were observed (eFigure 2A). The proportion of MuSCs entered into senescence was evaluated *via* the detection of beta-galactosidase activity and size of the cells ^{18, 24}. First, analysis of the cell size by flow cytometry showed an increase in the percentage of large cells in both sDM-, mDM- and jDM-MuSC populations, as

compared with HC-MuSCs (27.5, 24.6 and 35.1% of senescent cells, respectively, *versus* 18.2%) (Figure 4A). In all conditions, large cells showed an increase in beta-galactosidase activity, as compared with control (Mean Fluorescence Intensity (MFI) increased by 167, 159, and 139% respectively) (Figure 4B), accounting for a global increase of beta-galactosidase activity in the whole population. It was shown that in other contexts, such as aging and myotonic dystrophy type 2, human MuSCs that enter senescence do not proliferate and exhibit a deficit in implementing the myogenesis program, leading to less numerous and smaller myotubes^{25, 26}, as we observed here. In normal regenerating mouse muscle, the induction of senescence in MuSCs triggers an increased and sustained inflammation, leading to impaired muscle repair and fibrosis²⁷, as observed in sDM muscles. Interestingly, the analysis of the expression of myogenic factors *in vivo* in jDM showed that while the atrophic perifascicular areas are the place for an increased number of Pax7^{pos} cells, no increase of MyoD and myogenin positive cells is observed²², which is in accordance with our *in vitro* analysis.

These results point to augmented senescence in DM-MuSCs, which may explain their proliferation defect. *In vivo*, the accumulation of Pax7^{pos} cells in perifascicular areas may be due to activated MuSCs that cannot implement myogenesis due to proliferation defect because of entry into senescence. Thus, MuSCs get activated due to myofiber damage but their limited proliferative properties prevent efficient muscle repair. This is correlated with the severity of the disease and may account for the persistent muscle weakness observed in some sDM patients. We therefore investigated whether IFN-I plays a role in the proliferation deficit of DM-MuSCs.

Involvement of IFN-I in DM-MuSC proliferation deficit

High IFN-I level is a prominent feature in DM pathology and its expression in muscle and blood of patients is associated with the severity of the disease^{4, 6}. IFN-I involvement in DM and jDM pathogenesis has been confirmed by histological studies²⁸⁻³⁰, transcriptomic analyses^{31, 32}. Sources of IFN-I in DM skeletal muscle are diverse. Not only immune cells

express IFN-I, but endothelial cells, MuSCs themselves and newly formed myofibers^{14, 33}. The relative contribution of each cell type to the delivery of IFN-I in the neighboring milieu is not known, neither is the trigger leading to their expression/secretion of IFN-I. Nevertheless, we previously showed, using the SIMOA quantification, that jDM-MuSCs express IFN-I *in vitro* and that the expression is correlated with the severity of the disease¹⁴. Here, we evaluated the IFN score of adult DM-MuSCs through the quantification of the expression of 6 Interferon-stimulated genes (ISGs) using the Nanostring technology and found that the expression of IFIT44 and IFI27L was increased in sDM-MuSCs (eFigure 3B), confirming that IFN signaling occurred in these cells.

We therefore sought for a role of IFN-I pathway in the impaired MuSC proliferation in adult DM. First, we confirmed *in vivo* that IFN-signaling was operating in DM samples used in the present study. Myxovirus resistance protein A (MxA) is one of the IFN-I-inducible proteins^{2, 5, 30}. MxA immunoreactivity in the sarcoplasm of myofibers was detected in sDM, particularly in the perifascicular areas (eFigure 3C), as previously described^{5, 30}, *i.e.* in the areas where a higher number of Pax7^{pos} cells was found (see Figure 2). Therefore, upon myofiber injury, MuSCs get activated in an IFN-I enriched environment.

Functional investigation of IFN-I effects on MuSC proliferation was performed using gain- and loss-of-function experiments on MuSCs *in vitro*. Gain-of-function approach used the treatment of HC-MuSCs with escalating doses of human recombinant IFN- β . The lower dose tested (10 U/ml) induced an increase of 20% of MuSC proliferation while higher concentrations of IFN-I inhibited MuSC proliferation in a dose-dependent way to reach 35% of inhibition at 1000 U/ml (Figure 5A). This evokes an inhibitory effect of IFN-I on DM-MuSC proliferation at high concentrations. The inhibitory effect of IFN-I on the proliferation of various cell types is well documented³⁴ and MuSCs are no exception to the rule. Mechanistically, several studies reported that prolonged IFN-I stimulation triggers cellular senescence^{35, 36}. The link between IFN-I signaling, MuSC senescence and alteration of their proliferation deserves further investigation. However, it was shown that aged MuSCs reverse senescence and increase their proliferation, at the population level, if placed in an

environment stimulating their autophagy³⁷. Finally, IFN-I-driven alteration of MuSC proliferation impacts on their myogenesis potential. Accordingly, previous studies showed that treatment of mouse C2C12 cell line and healthy human MuSCs with high concentrations of IFN-I leads to the inhibition of myotube formation^{16, 38}.

In another series of experiments, we treated HC-MuSCs with conditioned medium prepared from growing sDM- or mDM-MuSCs and showed a decreased of their proliferation of 22 and 15%, respectively, as compared with conditioned medium prepared from HC-MuSCs (Figure 5B). This effect evidenced the autocrine nature of the deficit of proliferation observed in DM-MuSCs.

Loss-of-function experiments included the treatment of sDM-MuSCs with either Ruxolitinib, an inhibitor of the JAK/STAT pathway that equally inhibits JAK1, JAK2 and JAK3³⁹, or a blocking antibody against the IFN-I receptor (IFNAR) before testing their proliferation. Figure 5C shows that both treatments increased the proliferation of sDM-MuSCs by 190%, rescuing of the proliferative capacities of DM-MuSCs up to the range of HC-MuSCs (Figure 5B and 3B). This suggests that IFN-I is the main trigger of the proliferation defect observed in DM-MuSCs. To deepen this notion, we asked if Ruxolitinib could counteract the effects of the conditioned medium prepared from sDM-MuSC that was tested onto HC-MuSCs in Figure 3E above. Results in Figure 5D show that inhibiting IFN-signaling pathway rescued the inhibitory effect of the DM-MuSC supernatant (while no impact was observed with HC-MuSC supernatant). These data demonstrate that IFN-I secreted by DM-MuSCs is responsible for their low proliferation.

There are several evidence of IFN-I expression by MuSCs^{14, 40}, of their expression of ISGs (our results and^{41, 42}) and that Senescence-Associated Secretory Phenotype (SASP) includes IFN-I⁴³. Here, we show that autocrine/paracrine IFN-I delivery by DM-MuSCs is responsible of their myogenesis defect.

Conclusion

Our results show an unexpected and strong intrinsic alteration of proliferation of MuSCs in DM, which leads to impaired myogenesis *in vitro*. This is in accordance with the deficit in muscle repair observed in DM patient biopsies, and provides an explanation for the sustained muscle weakness that is observed in some severe forms of the disease. Indeed, though improvement of muscle capacities is observed after immunosuppressive treatment, some studies have shown that "despite all the immunosuppressive drugs prescribed, inflammatory myopathy patients rarely fully recover their initial strength" ^{8,9}.

IFN-I appears to be the main trigger of the alteration in sDM-MuSC proliferation since blocking this pathway blunts the proliferation deficit. Chronic inflammation reduces the proliferation and migration of neural stem cells ⁴⁴, blocks basal stem cells of the olfactory mucosa in the undifferentiated state through the IFN pathway ⁴⁵, and alters the balance and commitment of hematopoietic stem cell subsets ^{46, 47}. Here we propose that a sustained inflammatory environment triggers intrinsic changes in adult tissue stem cells, that affect their behavior through an autocrine/paracrine mechanism, including the sustained overexpression of IFN-I. Finally, our results advocate for the blockage of IFN-I signaling pathway in MuSCs to rewire myogenesis and muscle repair. In this respect, recent case reports presented encouraging results of the use of JAK/STAT inhibitors in severe DM or jDM patients ^{16, 48-50}.

Limitations of the study

There are several limitations to this study, and questions that it does not answer.

Intrinsic versus environmental causes of DM-MuSC proliferation defect. MuSCs from DM patients are exposed to chronic inflammation at the time of their isolation. The isolation procedure and cell culture duration exclude the presence of IFN coming from the *in vivo* environment of the cells. However, a sustained increase in IFN expression/secretion by MuSCs *in vitro* was observed by several studies ^{14, 40, 41, 42}, that is correlated with the severity of the disease in jDM ¹⁴. The *in vivo* environmental trigger of this increased IFN-I expression is not known (IFN or/and other factors), nor the duration of this effect, which would be hardly quantified experimentally.

Cell cycle and senescence in DM-MuSCs. DM being a chronic disease with repeated myofiber damages, MuSCs are constantly activated. An hypothesis would be that may exhaust the number of cycles there are capable of before entering into senescence. However, answering this question would require larger cohort of MuSC samples

Clinical relevance of the in vitro data. The small cohort of patient's material used in the present study prevents any clinical correlation, for instance in term of muscle damage, degree of muscle weakness, type of autoantibody, etc. Also the significance of the autocrine IFN-I loop in MuSCs is not possibly correlated with clinical parameters, due to the small number of patients. Larger cohort of patients would help to investigate the impact of the myogenesis deficit in DM patients from other parameters such as the response of the patients to immunosuppressive therapies.

Author contributions

Designing research studies: GM, BC

Conducting experiments: LG, LL, CF, MWG, SV

Analyzing data: NS, AC, CG, GM, BC

Writing the manuscript: LG, GM, BC

Editing the manuscript: all authors

Authors declare no conflict of interest

Acknowledgements:

This study was supported by Association Française contre les Myopathies-Telethon (Alliance MyoNeurALP), Société Française de Médecine Interne (support for LG) and Inserm (poste d'accueil for LG), and Fondation pour la Recherche Médicale (fellowship for LL). We thank the Laboratoire de Culture cellulaire du Service de Génétique et Biologie Moléculaire de l'Hôpital Cochin, Paris.

References

1. Pinal-Fernandez I, Mammen AL. Dermatomyositis etiopathogenesis: a rebel soldier in the muscle. *Curr Opin Rheumatol* 2018;30:623-629.
2. Benveniste O, Goebel HH, Stenzel W. Biomarkers in Inflammatory Myopathies-An Expanded Definition. *Front Neurol* 2019;10:554.
3. Ceribelli A, De Santis M, Isailovic N, Gershwin ME, Selmi C. The Immune Response and the Pathogenesis of Idiopathic Inflammatory Myositis: a Critical Review. *Clin Rev Allergy Immunol* 2017;52:58-70.
4. Arshanapalli A, Shah M, Veerula V, Somani AK. The role of type I interferons and other cytokines in dermatomyositis. *Cytokine* 2015;73:319-325.
5. Greenberg SA, Pinkus JL, Pinkus GS, et al. Interferon-alpha/beta-mediated innate immune mechanisms in dermatomyositis. *Ann Neurol* 2005;57:664-678.
6. Greenberg SA, Higgs BW, Morehouse C, et al. Relationship between disease activity and type 1 interferon- and other cytokine-inducible gene expression in blood in dermatomyositis and polymyositis. *Genes Immun* 2012;13:207-213.
7. Huard C, Gullà SV, Bennett DV, Coyle AJ, Vleugels RA, Greenberg SA. Correlation of cutaneous disease activity with type 1 interferon gene signature and interferon β in dermatomyositis. *Br J Dermatol* 2017;176:1224-1230.
8. Bronner IM, van der Meulen MF, de Visser M, et al. Long-term outcome in polymyositis and dermatomyositis. *Ann Rheum Dis* 2006;65:1456-1461.
9. Clarke AE, Bloch DA, Medsger TA, Jr., Oddis CV. A longitudinal study of functional disability in a national cohort of patients with polymyositis/dermatomyositis. *Arthritis Rheum* 1995;38:1218-1224.
10. Findlay AR, Goyal NA, Mozaffar T. An overview of polymyositis and dermatomyositis. *Muscle Nerve* 2015;51:638-656.
11. Winter A, Bornemann A. NCAM, vimentin and neonatal myosin heavy chain expression in human muscle diseases. *Neuropathol Appl Neurobiol* 1999;25:417-424.
12. Dumont NA, Wang YX, Rudnicki MA. Intrinsic and extrinsic mechanisms regulating satellite cell function. *Development* 2015;142:1572-1581.
13. Mammen AL, Allenbach Y, Stenzel W, Benveniste O. 239th ENMC International Workshop: Classification of dermatomyositis, Amsterdam, the Netherlands, 14-16 December 2018. *Neuromuscul Disord* 2020;30:70-92.
14. Gitiaux C, Latroche C, Weiss-Gayet M, et al. Myogenic Progenitor Cells Exhibit Type I Interferon-Driven Proangiogenic Properties and Molecular Signature During Juvenile Dermatomyositis. *Arthritis Rheumatol* 2018;70:134-145.
15. Ekholm L, Vosslander S, Tjärnlund A, et al. Autoantibody Specificities and Type I Interferon Pathway Activation in Idiopathic Inflammatory Myopathies. *Scand J Immunol* 2016;84:100-109.
16. Ladislau L, Suárez-Calvet X, Toquet S, et al. JAK inhibitor improves type I interferon induced damage: proof of concept in dermatomyositis. *Brain* 2018;141:1609-1621.
17. Abou-Khalil R, Le Grand F, Chazard B. Human and murine skeletal muscle reserve cells. *Methods Mol Biol* 2013;1035:165-177.
18. Debacq-Chainiaux F, Erusalimsky JD, Campisi J, Toussaint O. Protocols to detect senescence-associated beta-galactosidase (SA-beta-gal) activity, a biomarker of senescent cells in culture and in vivo. *Nat Protoc* 2009;4:1798-1806.
19. Pescarmona R, Belot A, Villard M, et al. Comparison of RT-qPCR and Nanostring in the measurement of blood interferon response for the diagnosis of type I interferonopathies. *Cytokine* 2019;113:446-452.
20. Varsani H, Charman SC, Li CK, et al. Validation of a score tool for measurement of histological severity in juvenile dermatomyositis and association with clinical severity of disease. *Ann Rheum Dis* 2015;74:204-210.
21. Wanschitz JV, Dubourg O, Lacene E, et al. Expression of myogenic regulatory factors and myo-endothelial remodeling in sporadic inclusion body myositis. *Neuromuscul Disord* 2013;23:75-83.

22. Baumann M, Gumpold C, Mueller-Felber W, et al. Pattern of myogenesis and vascular repair in early and advanced lesions of juvenile dermatomyositis. *Neuromuscul Disord* 2018;28:973-985.
23. Cseri K, Vincze J, Cseri J, et al. HMGB1 expression and muscle regeneration in idiopathic inflammatory myopathies and degenerative joint diseases. *J Muscle Res Cell Motil* 2015;36:255-262.
24. de Mera-Rodríguez JA, Álvarez-Hernán G, Gañán Y, Martín-Partido G, Rodríguez-León J, Francisco-Morcillo J. Is Senescence-Associated β -Galactosidase a Reliable in vivo Marker of Cellular Senescence During Embryonic Development? *Front Cell Dev Biol* 2021;9:623175.
25. Alsharidah M, Lazarus NR, George TE, Agle CC, Velloso CP, Harridge SD. Primary human muscle precursor cells obtained from young and old donors produce similar proliferative, differentiation and senescent profiles in culture. *Aging Cell* 2013;12:333-344.
26. Renna LV, Cardani R, Botta A, et al. Premature senescence in primary muscle cultures of myotonic dystrophy type 2 is not associated with p16 induction. *Eur J Histochem* 2014;58:2444.
27. Le Roux I, Konge J, Le Cam L, Flamant P, Tajbakhsh S. Numb is required to prevent p53-dependent senescence following skeletal muscle injury. *Nat Commun* 2015;6:8528.
28. Illa I, Gallardo E, Gimeno R, Serrano C, Ferrer I, Juárez C. Signal transducer and activator of transcription 1 in human muscle: implications in inflammatory myopathies. *Am J Pathol* 1997;151:81-88.
29. Salajegheh M, Kong SW, Pinkus JL, et al. Interferon-stimulated gene 15 (ISG15) conjugates proteins in dermatomyositis muscle with perifascicular atrophy. *Ann Neurol* 2010;67:53-63.
30. Uruha A, Allenbach Y, Charuel JL, et al. Diagnostic potential of sarcoplasmic myxovirus resistance protein A expression in subsets of dermatomyositis. *Neuropathol Appl Neurobiol* 2019;45:513-522.
31. Greenberg SA, Sanoudou D, Haslett JN, et al. Molecular profiles of inflammatory myopathies. *Neurology* 2002;59:1170-1182.
32. Rice GI, Melki I, Frémond ML, et al. Assessment of Type I Interferon Signaling in Pediatric Inflammatory Disease. *J Clin Immunol* 2017;37:123-132.
33. Tournadre A, Lenief V, Eljaafari A, Miossec P. Immature muscle precursors are a source of interferon- β in myositis: role of Toll-like receptor 3 activation and contribution to HLA class I up-regulation. *Arthritis Rheum* 2012;64:533-541.
34. Plataniias LC. Mechanisms of type-I- and type-II-interferon-mediated signalling. *Nat Rev Immunol* 2005;5:375-386.
35. Fu S, Wei J, Wang G, et al. The key role of PML in IFN- α induced cellular senescence of human mesenchymal stromal cells. *Int J Oncol* 2015;46:351-359.
36. Moiseeva O, Mallette FA, Mukhopadhyay UK, Moores A, Ferbeyre G. DNA damage signaling and p53-dependent senescence after prolonged beta-interferon stimulation. *Mol Biol Cell* 2006;17:1583-1592.
37. García-Prat L, Martínez-Vicente M, Perdiguero E, et al. Autophagy maintains stemness by preventing senescence. *Nature* 2016;529:37-42.
38. Franzi S, Salajegheh M, Nazareno R, Greenberg SA. Type 1 interferons inhibit myotube formation independently of upregulation of interferon-stimulated gene 15. *PLoS One* 2013;8:e65362.
39. Zhou T, Georgeon S, Moser R, Moore DJ, Caflisch A, Hantschel O. Specificity and mechanism-of-action of the JAK2 tyrosine kinase inhibitors ruxolitinib and SAR302503 (TG101348). *Leukemia* 2014;28:404-407.
40. Gitiaux C, Bondet V, Bekaddour N, et al. Inhibition of IFN α secretion in cells from patients with juvenile dermatomyositis under TBK1 inhibitor treatment revealed by single-molecular assay technology. *Rheumatology (Oxford)* 2020;59:1191.
41. Gallay L, Mouchiroud G, Chazaud B. Interferon-signature in idiopathic inflammatory myopathies. *Curr Opin Rheumatol* 2019;31:634-642.

42. Hou C, Durrleman C, Periou B, et al. From diagnosis to prognosis: Revisiting the meaning of muscle ISG15 overexpression in juvenile inflammatory myopathies. *Arthritis Rheumatol* 2021;73:1044-1052.
43. De Cecco M, Ito T, Petrashen AP, et al. L1 drives IFN in senescent cells and promotes age-associated inflammation. *Nature* 2019;566:73-78.
44. Pluchino S, Muzio L, Imitola J, et al. Persistent inflammation alters the function of the endogenous brain stem cell compartment. *Brain* 2008;131:2564-2578.
45. Chen M, Reed RR, Lane AP. Chronic Inflammation Directs an Olfactory Stem Cell Functional Switch from Neuroregeneration to Immune Defense. *Cell Stem Cell* 2019;25:501-513.
46. Esplin BL, Shimazu T, Welner RS, et al. Chronic exposure to a TLR ligand injures hematopoietic stem cells. *J Immunol* 2011;186:5367-5375.
47. Pietras EM, Mirantes-Barbeito C, Fong S, et al. Chronic interleukin-1 exposure drives haematopoietic stem cells towards precocious myeloid differentiation at the expense of self-renewal. *Nat Cell Biol* 2016;18:607-618.
48. Aeschlimann FA, Frémond ML, Duffy D, et al. A child with severe juvenile dermatomyositis treated with ruxolitinib. *Brain* 2018;141:e80.
49. Kahn JS, Deverapalli SC, Rosmarin DM. JAK-STAT signaling pathway inhibition: a role for treatment of discoid lupus erythematosus and dermatomyositis. *Int J Dermatol* 2018;57:1007-1014.
50. Le Voyer T, Gitiaux C, Authier FJ, et al. JAK inhibitors are effective in a subset of patients with juvenile dermatomyositis: a monocentric retrospective study. *Rheumatology (Oxford)* 2021: doi: 10.1093/rheumatology/keab1116.

Figure legends

Figure 1. Histology of mDM (mild dermatomyositis) and sDM (severe dermatomyositis) muscles. mDM muscles (left panel) showed a relatively preserved structure, with perivascular inflammatory infiltrates and slight perifascicular atrophy (arrow in Hematoxylin eosin [HE] staining), sparse myofibers undergoing regeneration (CD56 positive myofibers, arrow), and focal capillary drop out (asterisk in CD31 staining). sDM (right panel) showed important myofiber damage, large inflammatory infiltrates and severe perifascicular atrophy (arrows in HE staining), numerous myofibers undergoing regeneration with perifascicular enhancement (CD56 positive myofibers, arrows), and multiple and large capillary drop outs (asterisks in CD31 staining). Bar = 50 μ m.

Figure 2. *In vivo* muscle satellite cells in DM-MuSCs. *In vitro* immunofluorescence. Pax7^{pos} cells (arrows showing red labeling) in muscle sections of Healthy control (HC) and sDM muscle biopsies (laminin in green to delineate the myofibers, nuclei in blue). The graph on the right show the counting when discriminating perifascicular (2-3 first perifascicular myofibers) from intrafascicular (rest of the fascicule) areas (see example in eFigure 1). Student t-test. ***=p<0.001. Bars = 50 μ m.

Figure 3. *In vitro* myogenesis in DM-MuSCs. (A) Scheme of *in vitro* myogenesis (upper row) and of the culture assay set up (lower row) used for the experiments (representative pictures are provided in eFigure 2A). (B) Proliferation was evaluated as the percentage of Edu^{pos} cells. (C) Differentiation was evaluated as the percentage of Myogenin^{pos} cells. (D) Fusion index was evaluated as the percentage of nuclei within myotubes among the total number of nuclei. (E) Proliferation of jDM-MuSCs was evaluated as the percentage of Edu^{pos} cells and compared to age-matched HC-MuSCs. 5 HC-MuSCs, 5 sDM-MuSCs, 3 mDM-MuSCs, 3 young HC-MuSCs and 3 jDM-MuSCs were used. Statistical tests were implemented as follows: one-way Anova followed by Tukey's multiple comparison tests for B,C,D; Student t-test in G. *=p<0.05; **=p<0.01; ***=p<0.001; ****=p<0.0001.

Figure 4. Senescence in DM-MuSCs. Senescence of MuSCs was analyzed by flow cytometry. In (A), the percentage of large cells was evaluated among the whole population (representative dot plots are shown in the right where large cells are in upper right position in orange, small cells are in pink). In (B), the mean fluorescence intensity (MFI) for beta-galactosidase activity (C12FDG) is shown for each MuSC population (representative histograms are shown on the right with the threshold of the isotypic control in black). 5 HC-MuSCs, 4 sDM-MuSCs, 3 mDM-MuSCs and 3 jDM-MuSCs were used. Statistical tests

included one-way Anova followed by Tukey's multiple comparison tests. $^* = p < 0.05$; $^{**} = p < 0.01$; $^{***} = p < 0.0001$.

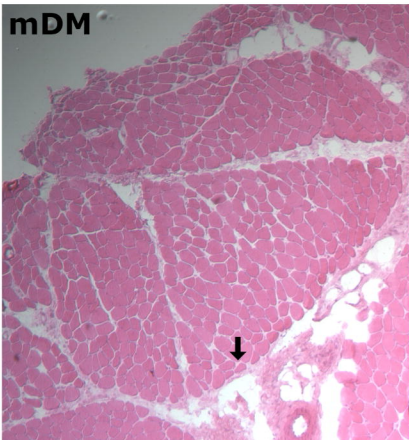
Figure 5. IFN-signaling in DM-MuSCs. **(A)** HC-MuSCs were treated with recombinant IFN-I at different concentrations. Each color indicates one HC-MuSC sample (5 HC-MuSCs were used). **(B)** HC-MuSCs were treated with conditioned medium from HC-, sDM- and mDM-MuSCs. Each symbol shape indicates the same HC-MuSC that was treated with different supernatants (3 different HC-MuSCs were used and treated with supernatants from 4 HC-MuSCs, 4 sDM-MuSCs, and 2 mDM-MuSCs). **(C)** sDM-MuSCs were treated with either a JAK inhibitor (Ruxolitinib) or a blocking antibody against IFN-I receptor (IFNAR). Each color indicates one sDM-MuSC sample (5 sDM-MuSCs were used). **(D)** HC-MuSCs were treated with conditioned medium from HC- or sDM-MuSCs with or without Ruxolitinib. Each color indicates the same HC-MuSC sample (4 different HC-MuSCs were used and treated with supernatants from 2 HC-MuSCs and 2 sDM-MuSCs). Statistical tests included one-way Anova followed by Tukey's multiple comparison tests. $^* = p < 0.05$; $^{**} = p < 0.01$; $^{***} = p < 0.001$.

Table 1. Histology and clinical score of DM patients

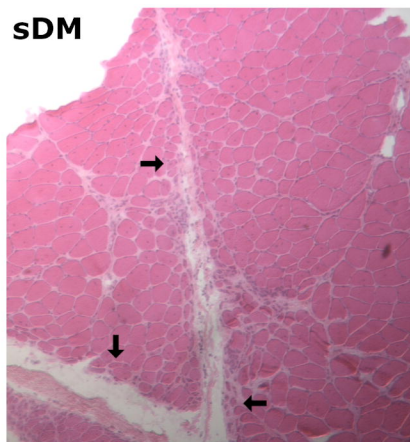
Patients	#1	#2	#3	#4	#5	#6	#7	#8
Inflammation								
Endomysial inflammatory infiltrates	0	0	1	2	1	1	1	1
Perimysial inflammatory infiltrates	0	0	0	2	2	2	0	1
Perivascular inflammatory infiltrates	0	1	0	2	2	2	1	2
Vessels								
Arterial abnormality	0	0	0	1	1	0	1	1
Myofibers								
Perifascicular myofiber atrophy	0	0	1	1	1	1	1	1
Non-perifascicular myofiber atrophy	0	0	1	1	1	1	1	1
Myofiber regeneration	0	1	1	1	1	1	1	1
Myofiber necrosis	0	0	0	1	1	1	1	1
Sarcolemmal C5b9 deposit	0	1	1	1	0	0	1	1
Central myonuclei in normal fibers	1	0	0	1	1	1	1	1
Interstitial compartment								
Endo- or perimysial fibrosis	0	0	0	1	1	1	1	1
Endo- or perimysial lipid deposits	0	0	0	0	0	1	0	1
Visual Analogic Scale score								
VAS	0.5	0.5	1	4	4	4	4	5
Histological DM severity score	1.5	3.5	6	18	16	16	14	18
Classification								
	mDM	mDM	mDM	sDM	sDM	sDM	sDM	sDM
Clinical characteristics								
	#1	#2	#3	#4	#5	#6	#7	#8
Sex	M	M	F	M	F	F	M	F
Age (years)	66	39	72	63	57	23	59	28
Diagnosis delay (months)	9	12	38	13	10	4	6	8
Time from onset to last follow up (y)	6	3	3	4	9	2	4	3
Last MRC testing (scale 0-5)	5	5	5	4	4	4	4	4
Worst MRC testing (scale 0-5)	5	5	4	3	4	4	4	4
Proximal/distal muscle weakness	/	/	prox.	prox.	prox.	prox.	prox.	prox.
Persistence of muscle weakness*	no	no	no	yes	yes	yes	yes	yes
Walking aid device requirement	no	no	no	yes	no	no	no	yes
Swallowing disorder	no	no	no	yes	yes	yes	yes	no
Maximal creatine kinase (UI/L)	400	300	930	560	780	1200	6500	370
Aldolase (UI/L)	12.4	20	24.5	9.9	5.5	46	/	17
Specific auto-antibody	MDA5	MDA5	Mi2	/	MDA5	Mi2	SAE2	MDA5
Muscle biopsy site	Delt.	Quad.	Quad.	Delt.	Delt.	Delt.	Quad.	Delt.

*mDM: mild dermatomyositis; sDM: severe dermatomyositis; F: Female, M: Male, MRC testing (Medical research Council score); *: at last follow-up; prox: proximal; Delt.: deltoid; Quad.: quadriceps.*

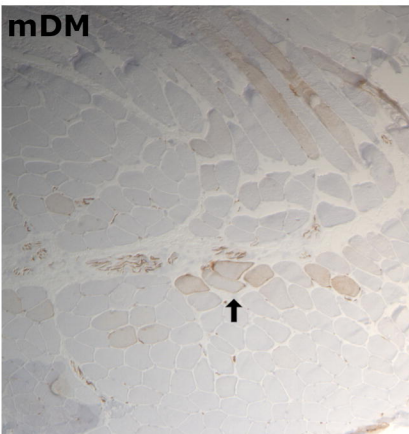
HE



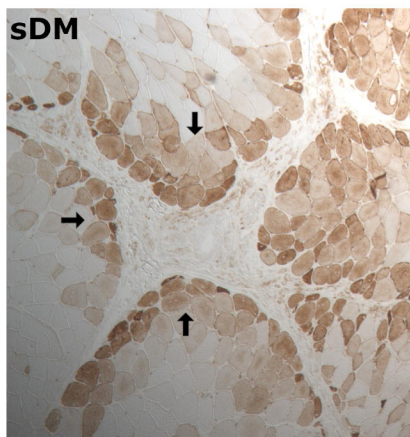
sDM



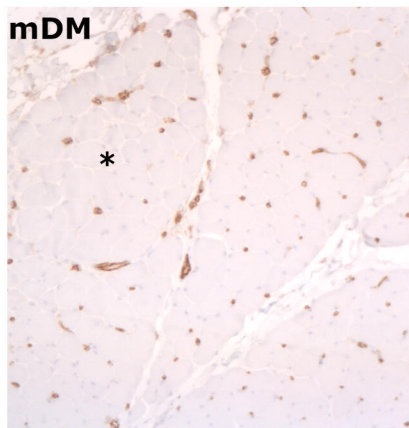
CD56



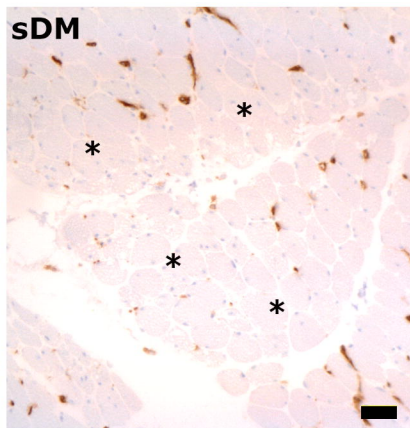
sDM

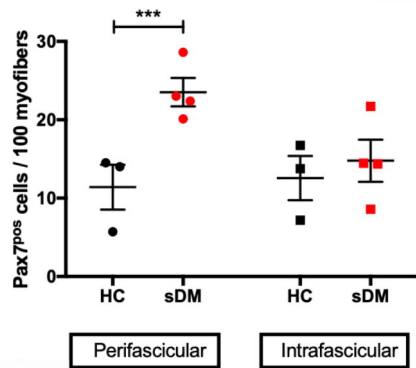
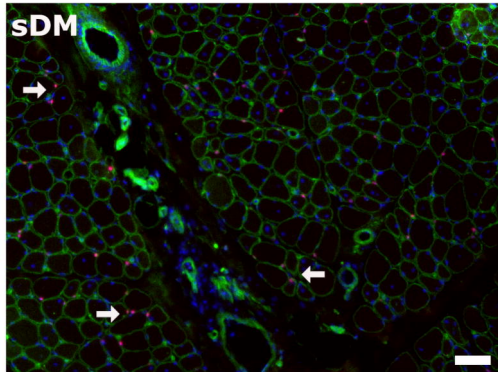
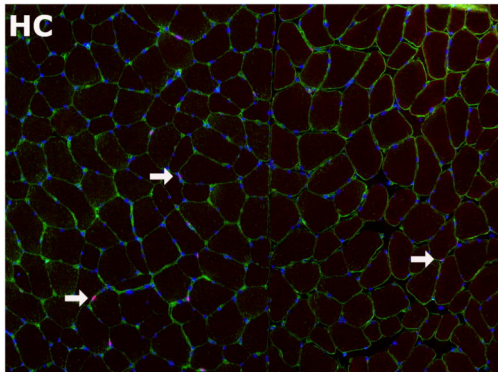


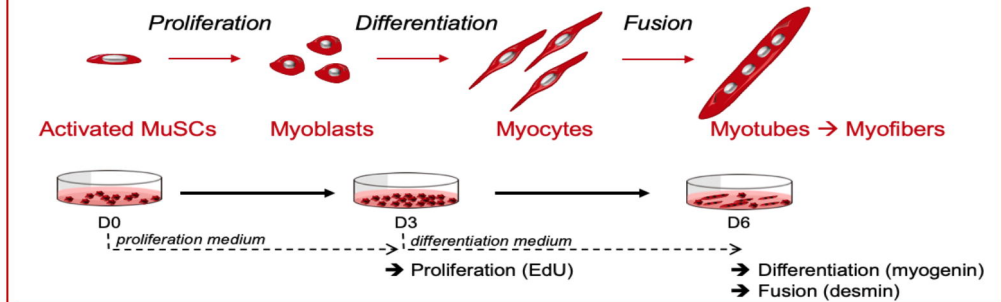
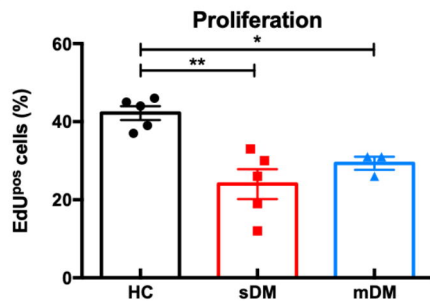
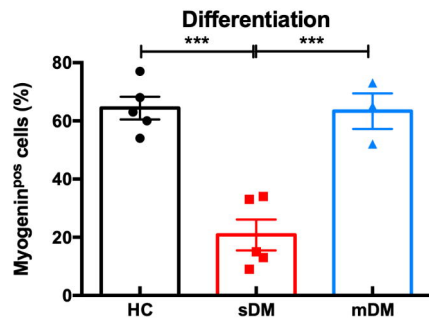
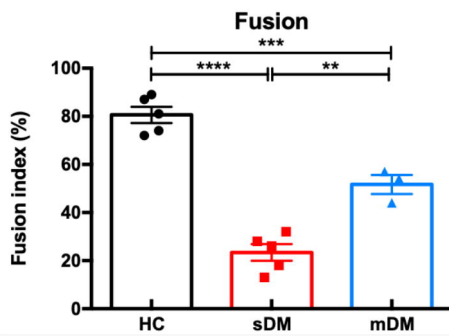
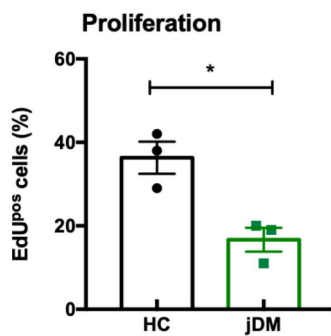
CD31

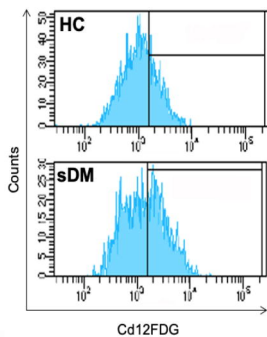
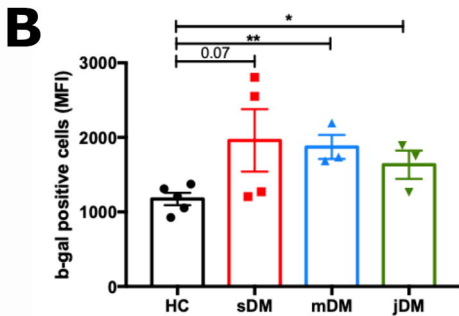
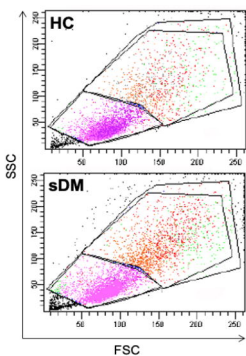
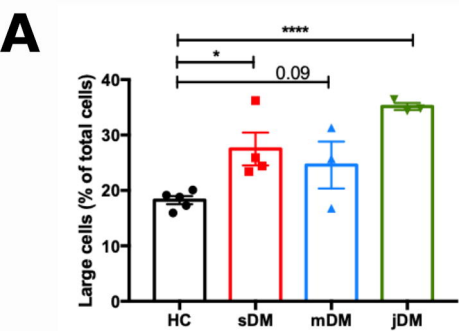


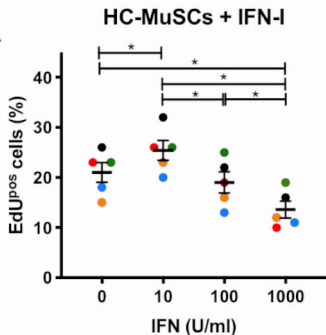
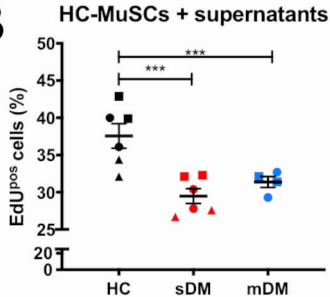
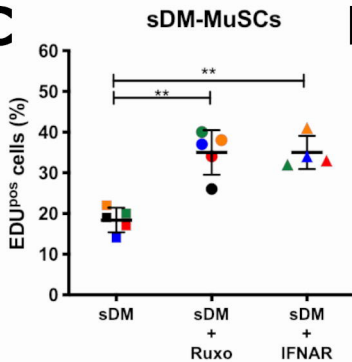
sDM





A**B****C****D****E**



A**B****C****D**